Proceedings of the
44th IEEE Conference on Decision and Control, and
the European Control Conference 2005
Seville, Spain, December 12-15, 2005



# Observer based imaging methods for Atomic Force Microscopy

Deepak R. Sahoo, Tathagata De and Murti V. Salapaka,
NanoDynamics Systems Lab,
Department of Electrical & Computer Engineering,
Iowa State University, Ames, Iowa, USA, 50011.

***Abstract*— In atomic force microscopy, bandwidth or resolution can be affected by active quality factor ($Q$) control. However, in existing methods the trade off between resolution and bandwidth remains inherent. Observer based $Q$ control method provides greater flexibility in managing the tradeoff between resolution and bandwidth during imaging. It also facilitates theoretical analysis lacking in existing methods.**

**Steady state signals like amplitude and phase are slowly varying variables that are suited to image low bandwidth content of the actual sample profile. Observer based transient imaging scheme with $Q$ control has the promise of detecting high bandwidth content of the sample features during scanning. Transient detection also has the advantage of high sensitivity to small features.**

## I. INTRODUCTION

There is considerable interest in interrogation and manipulation of surface properties of inorganic and biological materials at molecular level using atomic force microscope (AFM) [1]. AFM is often operated in the dynamic mode (i.e. amplitude modulation and frequency modulation) to image with low lateral force and high force sensitivity. A schematic of AFM operating in dynamic mode is shown in Fig. 1. In this mode of operation a sinusoidal excitation is applied by the dither piezo at the base of the cantilever. The tip of the oscillating cantilever interacts with the sample. The cantilever tip deflection is measured by a photo diode. A set point amplitude of the deflection signal is maintained by feeding back the amplitude signal to the sample positioning system (z-piezo). The sample is raster scanned by the XY-scanner. During imaging the effective spring constant and damping coefficient of the cantilever change due to interaction with the sample. In amplitude modulation method the control signal and the amplitude and phase of the cantilever deflection signal during scanning is used to construct the image of the sample.

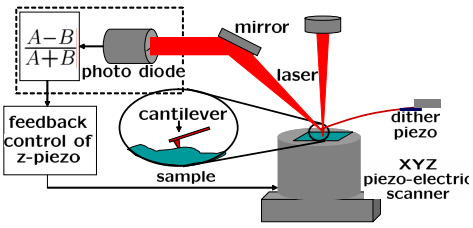


Fig. 1. A schematic of AFM.

The scan speed in atomic force microscopy is dictated by the mechanical bandwidth of the z-piezo and the cantilever. High quality factor ($Q$) of the cantilever gives better imaging resolution. However, high $Q$ results in large settling times for the amplitude and phase signals. Thus imaging speed of methods based on amplitude regulation is compromised by high quality factor $Q$.

Recently several methods have been proposed to increase the bandwidth or the resolution of imaging in dynamic mode atomic force microscopy. In [2], while imaging in air the scan speed is increased by using a z-piezo with high bandwidth and by active $Q$ reduction of the cantilever. In [3] the force sensitivity (resolution) is enhanced by 3 orders of magnitude by active $Q$-enhancement of the cantilever. Given a z-piezo with a high mechanical bandwidth, in dynamic methods, the bandwidth and resolution of imaging is dictated by the quality factor $Q$ of the cantilever.

Imaging under fluids with $Q$-enhancement has numerous advantages. While imaging in air, molecular forces (in piconewton range) are not accessible due to capillary forces (in nanonewton range) from the moisture layer present on the sample. On the contrary atomic resolution images have been obtained with imaging under fluid [4]. The biological samples are soft and they often need to be imaged in a buffer solution. The low lateral forces in fluids facilitates imaging of biological sample as they are not displaced or destroyed [5], [6]. However, under fluids the quality factor and the force sensitivity of the cantilever is reduced by approximately two orders of magnitude compared to their value in air. Therefore it is essential to actively enhance the $Q$ of cantilever and consequently the force sensitivity in order to sense molecular level forces. In [3] the $Q$ is enhanced by three orders of magnitude and correspondingly the force sensitivity is improved to piconewton regime.

In the existing methods of $Q$-control, the deflection signal is phase shifted (or time delayed) and amplified before adding it to the standard excitation signal. However, in this method the trade off between bandwidth and resolution remains inherent [7]. It is always desirable to improve both bandwidth and resolution together. In the current methods the feedback loop is fixed and the resolution and bandwidth are fixed according to a single parameter: the effective $Q$. Observer based $Q$ control method provides flexibility in the feedback loop to improve resolution in the case of active damping or improve bandwidth in the case of $Q$-

0-7803-9568-9/05/$20.00 ©2005 IEEE

enhancement.

Another advantage of observer based approach is its amenability to the transient detection technique. Note that imaging signals like the amplitude and phase being slow varying, are inadequate to construct the high bandwidth (fine) features of sample surface. Based on these methods, at higher scan rates or scan sizes the sample features appear at higher temporal frequency to the cantilever and the image may not portray the fine features on the sample. On the other hand, transient detection method in [8] is able to detect tip-sample interactions at a very high bandwidth (not limited by high $Q$). Transient detection method adapted to sample imaging with observer based $Q$ control can detect high bandwidth content of the sample at high scan rates that is not possible with amplitude and phase based imaging schemes.

## II. Observer based imaging

### A. AFM model

From a system perspective, the input signal to AFM is the excitation signal applied to the dither-piezo and the output signal is the deflection of the cantilever-tip obtained from the photo-diode. The frequency of the excitation signal is close to the first resonant frequency of the cantilever. It is experimentally observed that near the first resonant frequency, the transfer function from the dither-piezo-input to the photo-diode-output is described by a second order model with a right half plane zero, given by:

$$G(s) = \frac{k/m(c_1 + c_2 s)}{s^2 + \frac{\omega_0}{Q} s + \omega_0^2}, \tag{1}$$

where $k$, $m$, $\omega_0$ and $Q$ are the equivalent stiffness, equivalent mass, resonance frequency in $rad/sec$ and quality factor of the cantilever. Note that $k/m = \omega_0^2$. By putting $c_1 = 1$ and $c_2 = 0$ in Eq.(1), the traditionally employed transfer function corresponding to the point mass description of the cantilever is obtained.

In AFM setup, as described in Fig. 2, the thermal noise $\eta$ enters as a process noise, the photo-diode noise appears at the output as a measurement noise and the tip-sample force appears at the input of the cantilever. A state-space representation of AFM is given by,

$$\begin{array}{rcl} \dot{x} & = & Ax + Bu + B_1 h + B_1 \eta;\ x(0) = x_0, \\ y & = & Cx + \upsilon, \end{array} \tag{2}$$

where state matrices $A$, $B$, $B_1$ and $C$ are realized from the frequency response from dither-piezo-input to photo-diode-output. $x$ is the dynamic state of the cantilever, $u$ is the dither-piezo-input and $y$ is the photo-diode-output. The canonical realization of the transfer function (fitted to the frequency response of AFM) in Eq.(1) gives $A = [0, 1; -\omega_0^2, -\omega_0/Q]$, $B = [0; k/m]$, $B_1 = [0; 1/m]$ and $C = [c_1,\ c_2]$. Cantilever-tip position $p = Cx$ and velocity $v = [0,\ 1]x$.

The tip-interaction force $h$ is a function of tip position $p$ and the velocity $\dot{p}$, i.e. $h = \Phi(p, \dot{p})$. The function $\Phi$ is a nonlinear function of $p$ and depends on the sample. Thus in presence of sample the interconnection as of the cantilever and the sample is described by:

$$\begin{array}{rcl} p & = & \Phi_{hp} h + \Phi_{gp} g, \\ h & = & \phi(p, \dot{p}), \end{array}$$

where $\Phi_{hp}$ and $\Phi_{gp}$ are the maps from $h \rightarrow p$ and $g \rightarrow p$, respectively. $g$ is typically a sinusoidal input to the dither-piezo. This feedback interconnection is evidently quite complex. However, by treating $h$ as an independent input to the cantilever, qualitative arguments about bandwidth and resolution during imaging can be obtained and verified through simulation.

### B. Observer model

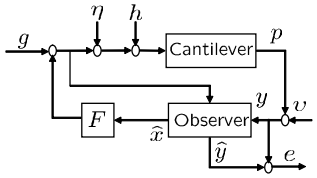


Fig. 2. The block diagram of AFM combined with observer.

An observer is designed based on the AFM model given by Eq.(2) that provides the estimated position $\hat{p}$ and velocity $\hat{v}$ of the cantilever tip. The block diagram of AFM combined with an observer is given in Fig. 2. In observer based $Q$ control paradigm $\hat{p}$ and $\hat{v}$ are added in feedback to the standard excitation signal $g$ to actively damp or enhance the $Q$ of the cantilever. The observer dynamics is given by:

$$\begin{array}{rcl} \dot{\hat{x}} & = & A\hat{x} + Bu + L(y - C\hat{x});\ \hat{x}(0) = \hat{x}_0, \\ u & = & (g + F\hat{x}), \\ \hat{p} & = & C\hat{x}, \\ \hat{v} & = & D\hat{x}, \end{array} \tag{3}$$

where $L$ is the observer gain and $F$ is the state feedback gain.

Let $\tilde{x} = x - \hat{x}$ denote the state estimation error. The combined cantilever-observer dynamics is given by,

$$\begin{array}{rcl} \begin{bmatrix} \dot{x} \\ \dot{\tilde{x}} \end{bmatrix} & = & \begin{bmatrix} A + BF & -BF \\ 0 & A - LC \end{bmatrix} \begin{bmatrix} x \\ \tilde{x} \end{bmatrix} + \\ & & \begin{bmatrix} B \\ 0 \end{bmatrix} g + \begin{bmatrix} B_1 \\ B_1 \end{bmatrix} (h + \eta) - \begin{bmatrix} 0 \\ L \end{bmatrix} \upsilon, \\ \begin{bmatrix} y \\ \hat{p} \\ \hat{v} \end{bmatrix} & = & \begin{bmatrix} C & 0 \\ C & -C \\ D & -D \end{bmatrix} \begin{bmatrix} x \\ \tilde{x} \end{bmatrix} + \begin{bmatrix} 1 \\ 0 \\ 0 \end{bmatrix} \upsilon. \end{array} \tag{4}$$

### C. Estimated state feedback

It can be shown from Eq.(4) that the transfer function from the excitation signal $g$ to the cantilever-tip deflection signal $y$ is given by:

$$\begin{array}{rcl} (g \rightarrow y)(s) & = & C[sI - (A + BF)]^{-1} B \\ & = & \frac{k/m(c_1 + c_2 s)}{s^2 + s\frac{\omega_{qc}}{Q_{qc}} + \omega_{qc}^2}, \end{array} \tag{5}$$

where $F = [F_1,\ F_2](m/k)$, $\frac{\omega_{qc}}{Q_{qc}} = \frac{\omega_0}{Q} - F_2$ and $\omega_{qc}^2 = \omega_0^2 - F_1$. Note that $\omega_{qc}$ and $Q_{qc}$ are the modified resonant frequency and quality factor of the cantilever.

In Eq.(5) $(g \to y)(s)$ is an exact second order transfer function. It is independent of observer gain $L$. In this paradigm the modified transfer function has the same structure as the unmodified transfer function (compare Eq.(1) with Eq.(5)) with an equivalent quality factor $Q_{qc}$ and equivalent resonant frequency $\omega_{qc}$. Thus one can imagine the new dynamics is to mimic the dynamics of a new enhanced cantilever with changed quality factor $Q_{qc}$ and changed resonant frequency $\omega_{qc}$. This provides considerable advantages in analyzing the $Q$ controlled dynamics. It needs to be noted that the equivalent transfer function is not higher order; in the above architecture suitable pole-zero cancelation has taken place to obtain a second order description of the closed-loop system even though the state space dimension is four. However $(g \to y)(s)$ in existing methods (with a phase shifter or time delay implemented into the feedback architecture) is a high order or an infinite dimensional system [9]. Therefore in existing methods one has to *approximate* the resulting transfer function to a second-order behavior with the purpose of carrying the intuition of a modified cantilever to the interpretation of the cantilever-sample interconnection.

In existing methods assumption is made that the cantilever is a second order transfer function with a constant numerator and the cantilever deflection is purely sinusoidal so that a 90 degrees phase shift yields the velocity of the cantilever. Both these assumptions typically do not hold. In the proposed method the feedback signal is the *estimated* tip-velocity. From Eq.(5) it can be seen that by appropriately choosing $F$ a desired quality factor and resonance frequency of the cantilever can be obtained. Note that $\omega_{qc}^2 = \sqrt{k_{qc}/m}$, $k_{qc}$ being the modified stiffness of the cantilever. Therefore a desired stiffness of the cantilever can be obtained by feeding back the estimated tip position signal. By varying $F_2$ only the desired quality factor can be achieved independently. Active $Q$ control of the cantilever by feeding back the estimated tip velocity (i.e. $F_1 = 0$) is considered.

When the cantilever is not interacting with the sample, the bandwidth is entirely determined by the transfer function $(g \to y)(s)$ as $h = 0$. Note that $F$ can be chosen to determine the cantilever off-sample behavior. Typically, one would need large damping (low $Q_{qc}$) off sample. Resolution does not have any significance and therefore high bandwidth is the only objective. The on-sample behavior is analyzed next.

### *D. Effect of tip-sample force*

The effect of tip-sample force $h$ on tip deflection $y$ during imaging is given by the transfer function:

$$\begin{aligned}(h \to y)(s) &= C[sI - A_{BF}]^{-1}B_1 - \\ &\quad C[sI - A_{BF}]^{-1}BF[sI - A_{LC}]^{-1}B_1, \\ &= \frac{1/m(c_1 + c_2 s)}{s^2 + s\frac{\omega_{qc}}{Q_{qc}} + \omega_{qc}^2} \times \\ &\quad \left[1 - \frac{F_1(1 - l_1c_2) + F_2(s + l_1c_1)}{s^2 + s\frac{\omega_{kf}}{Q_{kf}} + \omega_{kf}^2}\right],\end{aligned} \tag{6}$$

where $A_{BF} = A + BF$, $A_{LC} = A - LC$, $\frac{\omega_{kf}}{Q_{kf}} = \frac{\omega_0}{Q} + l_1c_1 + l_2c_2$ and $\omega_{kf}^2 = \omega_0^2(1 - l_1c_2) + l_1c_1\frac{\omega_0}{Q} + l_2c_1$.

The bandwidth and resolution during imaging depends on the maps $(h \to y)(s)$ and $(g \to y)(s)$. If the gain of $(h \to y)(s)$ is large, the effect of $h$ on $y$ is large and consequently the resolution is high. If the bandwidth of $(h \to y)(s)$ is high, the tip deflection due to $h$ settle down fast and consequently the bandwidth is high. From Eq.(6) it follows that as L is increased from 0 to high values $(h \to y)(s)$ changes from the uncontrolled original cantilever dynamics to given in Eq.(1) to modified dynamics given in Eq.(5). Thus, by an approximate choice of $L$, one can achieve entire range of sample behavior that differs from off-sample behavior. In effect observer based methodology provides a "dual $Q$" control; (a) choice of $F$ determines off-sample behavior and (b) choice of $L$ determines on-sample behavior.

Observer based $Q$ control for active damping in air and $Q$ enhancement in water is considered. The benefits of observer based $Q$ control in AFM imaging by using smaller observer gain $L$ is presented. The models are derived from experimental data.

A cantilever having $f_0 = 68.1$ kHz while oscillating in air with $Q = 200$ is damped by 10 times to $Q_{qc} = 20$ by choosing $F = k/m[0, 9\omega_0/Q]$. $(h \to y)(s)$ for different values of observer gain $L$ is plotted in Fig. 3(a). As the values of $L$ increases, $(h \to y)(s)$ approaches $(g \to y)(s)/k$. By choosing smaller values of $L$ the effect of tip-sample forces on tip deflection $y$ can be enhanced. In Fig. 3(c) the amplitude of deflection signal $y$ is plotted when the cantilever encounters a step sample profile of 5 nm height between time instants 6000 $\mu$sec and 8000 $\mu$sec while freely oscillating at 24 nm. For smaller values of $L$ the cantilever settles down to a lower amplitude further away from the sample compared to larger values of $L$. The tip-sample interaction force is smaller for smaller $L$. Thus a higher force sensitivity and resolution can be achieved by using a smaller value for $L$ without compromising the off-sample bandwidth. When the step sample profile goes away at 8000 $\mu$sec i.e. $h = 0$, the deflection signal builds up to the free oscillation amplitude at the desired bandwidth. Thus one can conclude that at a given scan speed and increase in bandwidth by active damping, the resolution can be improved by choosing smaller value for $L$.

In another experiment, the $Q$ of a cantilever ($f_0 = 16$ kHz) oscillating under water with $Q = 40$ is enhanced by 10 times to $Q_{qc} = 400$ by choosing $F = k/m[0, -0.9\omega_0/Q]$. $(h \to y)(s)$ for different values of observer gain $L$ is plotted in Fig. 3(b). As $L$ is increased, $(h \to y)(s)$ approaches $(g \to y)(s)/k$ from below. By choosing smaller values of $L$ a better bandwidth can be obtained in presence of tip-sample force $h$. In Fig. 3(d) the amplitude of the deflection signal $y$ is plotted when the cantilever encounters a step sample profile of 5 nm height between time instants of 40 ms and 70 ms while freely oscillating at 40 nm. For smaller value of $L$ the cantilever takes shorter time to settle down over the sample. Due to high $Q$ the cantilever settles down to the attractive regime of the sample where $h$ is small. Therefore the difference in amplitudes is small for different values

of $L$. By choosing small value for $L$ the force sensitivity or resolution is not compromised; however the bandwidth is enhanced in presence of sample. When the step sample profile goes away at 70 ms i.e. $h = 0$, the deflection signal builds up to the free oscillation amplitude at the bandwidth corresponding to the $Q$ enhancement. The phase of the deflection signal $y$ shows a similar behavior as the amplitude signal. The simulation shows that at a given scan speed and $Q$ enhancement, the bandwidth can be improved by choosing smaller value for $L$.

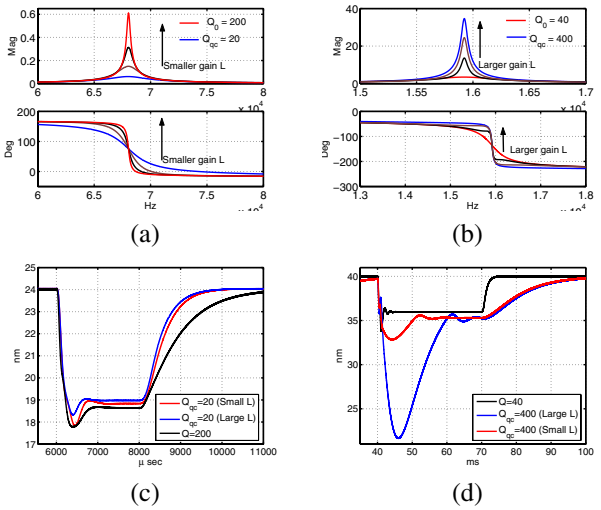


Fig. 3. The transfer function from tip-sample interaction $h$ to deflection signal $y$ is plotted for different values of observer gain $L$ when the cantilever is oscillating (a) in air and it is actively damped and (b) under water and the $Q$ is enhanced. The amplitude signal for small and large values of $L$ is plotted in (c) and (d) corresponding to (a) and (b) when the cantilever encounters a step sample profile while freely oscillating in air and under water, respectively.

### *E. Effect of noise*

The effect of thermal noise $\eta$ and photo-diode noise $\upsilon$ on the deflection signal $y$ is given by the transfer functions:

$$(\eta \rightarrow y)(s) = C[sI - A_{BF}]^{-1}B_1 - C[sI - A_{BF}]^{-1}BF[sI - A_{LC}]^{-1}B_1, \quad (7)$$

and

$$(\upsilon \rightarrow y)(s) = 1 + C[sI - A_{BF}]^{-1}BF[sI - A_{LC}]^{-1}L \quad (8)$$

respectively.

The effect of thermal noise $\eta$ and photo-diode noise $\upsilon$ on estimated cantilever-tip position $\hat{p}$ is given by the transfer functions:

$$(\eta \rightarrow \hat{p})(s) = C[sI - A_{BF}]^{-1}L - C[sI - A_{LC}]^{-1}B_1 - C[sI - A_{BF}]^{-1}BF[sI - A_{LC}]^{-1}B_1 \quad (9)$$

and

$$(\upsilon \rightarrow \hat{p})(s) = C[sI - A_{LC}]^{-1}L + C[sI - A_{BF}]^{-1}BF[sI - A_{LC}]^{-1}L \quad (10)$$

respectively.

The severity of the effect of thermal noise $\eta$ and photo-diode noise $\upsilon$ on deflection signal $y$ and tip-position estimate $\hat{p}$ is obtained by analyzing Eq.(7), (9), (8) and (10) for different values of gain $F$ and $L$. It can be shown that if the cantilever is actively damped (i.e. $\omega_{qc}/Q_{qc}$ is increased) the effects of thermal noise and photo-diode noise in deflection signal and tip position estimate are reduced. In the case of $Q$-enhancement of the cantilever the effect of thermal noise and photo-diode noise is also enhanced in deflection signal and tip position estimate. From Eq.(9) and (10) it can be shown that the noise effect further reduces in $\hat{p}$ by choosing smaller values of $L$ for both damping and $Q$ enhancement scenario.

In Fig. 4(a) and (c) the thermal noise power and photo-diode noise power in $y$ and $\hat{p}$ respectively are shown when the cantilever is oscillating in air. It is observed that when the cantilever is damped by an order of magnitude the noise contribution is also reduced by an order of magnitude. In Fig. 4(b) and (d) the thermal noise power and photo-diode noise power in $y$ and $\hat{p}$ respectively are shown when the cantilever is oscillating in water. It is observed that when quality factor of the cantilever is enhanced by 4 times in its magnitude the noise contribution increase by over an order of magnitude. Therefore the thermal noise and more prominently the photo-diode noise may have drastic effects while imaging under fluid with large $Q$ enhancement.

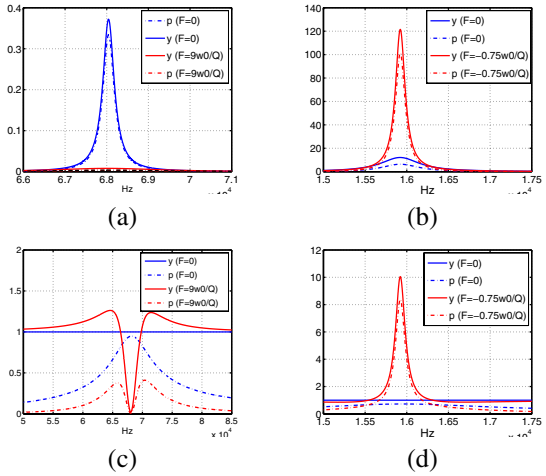


Fig. 4. The transfer function from thermal noise $\eta$ and photo-diode noise $\upsilon$ to deflection signal $y$ and tip position estimate $\hat{p}$ are plotted when the cantilever is oscillating in air and damped (a) and (c) and when the cantilever is oscillating in water and $Q$ enhanced (b) and (d).

### *F. Imaging with transient detection*

Observer based imaging has numerous benefits with respect to resolution, bandwidth and noise reduction. However the imaging signals i.e. the amplitude and phase of deflection signal $y$ and estimated tip position $\hat{p}$ remain slow. Therefore at a given scan speed these signals represent a low bandwidth content (slow varying features) of the actual sample profile. As the scan speed is increased the image looks smoother and the fine details of the sample is lost. The transient

detection technique has promise of detecting high bandwidth content of sample profile. Even small tip-sample interactions corresponding to sub-nanometer level sample features can also be detected with a high probability. We consider the transient detection scheme with $Q$-control in true imaging scenario.

The effect of excitation signal $g$ on innovation signal $e = y - C\hat{x}$ is given by the transfer function: $(g \to e)(s) = 0$. The effect of tip-sample interaction force $h$ on innovation signal $e$ is given by the transfer function:

$$\begin{aligned}(h \to e)(s) &= C[sI - (A - LC)]^{-1}B_1, \\ &= \frac{1/m(c_1 + c_2 s)}{s^2 + s\frac{\omega_{kf}}{Q_{kf}} + \omega_{kf}^2}. \end{aligned} \quad (11)$$

The transient signal is not affected by the choice of $F$. The transient detection scheme can be implemented independent of the $Q$-control scheme. It can be shown from Eq.(11) that the bandwidth of detecting tip-sample interaction ($BW_{kf} \propto \frac{\omega_{kf}}{Q_{kf}}$) can be enhanced which is independent of $Q$ [8].

## III. Experimental Results

In the experiments the frequency response of the AFM setup is obtained via a HP 3563A control system analyzer. A model of the AFM is obtained from the frequency response data.

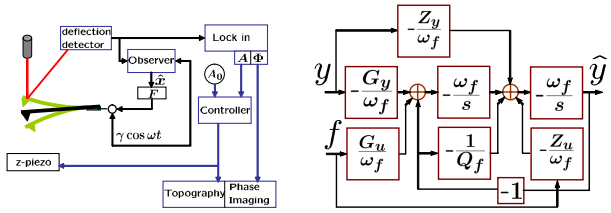


(a) (b)

Fig. 5. (a) An observer is implemented into the standard tapping mode imaging set up. The state estimates are used for $Q$-control and imaging. (b) The observer is implemented as an analog circuit (Tow-Thomas biquad). It has a second order transfer function with gain $G_u$ and a right half plane zero $Z_u$ from input $u$, and gain $G_y$ and a left half plane zero $Z_y$ from input $y$. $\omega_f$ and $Q_f$ are the resonant frequency and quality factor of the observer. A similar circuit is implemented that gives the cantilever-tip velocity estimate $\hat{v}$.

The noise in the measurement and the thermal noise are experimentally found out. The measurement noise (mainly photo-diode noise) is quantified from the deflection signal when the cantilever is forced to remain in contact with a hard sample surface. The thermal noise is measured from the deflection signal of freely oscillating cantilever with no excitation signal ($g = 0$).

Conventional tapping mode AFM set up with an observer is shown in Fig. 5(a). This setup is used for observer based imaging experiments presented in this paper. The cantilever is excited near its resonance frequency with $g = \gamma \cos \omega t$. A PI controller actuates the vertical piezo to move the sample to maintain a constant set-point amplitude ($A_0$). The observer provides the estimates of the cantilever tip position and velocity. The effective quality factor of the cantilever is regulated by feedback gain $F$.

### A. Observer based $Q$-control

The experimental result of $Q$-enhancement under water is presented. In this experiment a soft cantilever (Olympus Biolever-B) with resonant frequency $f_0 = 16$ kHz, nominal quality factor $Q = 5$ and stiffness $k = 0.005$ N/m in water is used with the Asylum Research MFP3D afm. The frequency response of the AFM set up shows forest of peaks due to response of the cantilever to the acoustic excitation due to the surrounding fluid motion. A second order transfer function with a right half plane zero is fit to the frequency response data. The frequency response and the fitted transfer function is shown in Fig. 6(a). An observer for this system is designed and implemented in an analog circuit as shown in Fig. 5(b). By increasing the observer gain $F$, quality factor of the cantilever is experimentally increased to 350 under water. Gradual increase in $Q$ by observer based $Q$-control is shown in Fig. 6(b).

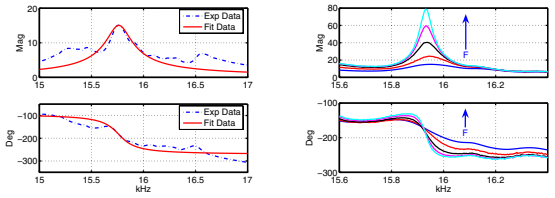


(a) (b)

Fig. 6. (a) The frequency response of the cantilever under water is modeled as a second order transfer function with a right half plane zero. The model has first resonant frequency at 15.9 kHz, quality factor $Q = 37.3$ and phase offset $\phi = 42°$. (b) The frequency response of the cantilever is plotted when the feedback gain $F$ is gradually increased.

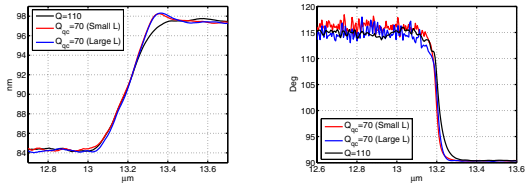


(a) (b)

Fig. 7. (a) The amplitude of the deflection signal. (b) The phase of the deflection signal. The cantilever comes off the step in the calibration sample near 13 $\mu$m.

In another experiment the cantilever with $f_0 = 68.1$ kHz is damped from $Q = 110$ to $Q_{qc} = 70$ in air. A model is obtained from the frequency response data and an analog Kalman filter is implemented. The amplitude and phase profile is plotted in Fig. 7 for different values of $L$ when the cantilever was coming off a 20 nm step on a grating sample. The free oscillation amplitude was 97.3 nm and set point amplitude was 87.3 nm with feedback gain $K_p = 0$ and $K_i = 0.2$ on the z-piezo. It can be seen that the amplitude and phase builds to free oscillation amplitude and phase values faster when the cantilever is damped. The rate of growth of amplitude and phase profile off-sample is equal for different values of $L$. The simulation of the experiment revealed smaller tip-sample interaction force for smaller

value of $L$. Experimental transfer function $(h \rightarrow y)(s)$ for different values for $L$ is obtained with the sample force $h$ provided by a signal generator. The on-sample behavior is under experimental investigation.

### B. Imaging with transient detection

In this experiment a Digital Instruments multi-mode afm with an extender and signal access module was used. A Kalman observer is designed from a second order model obtained from the frequency response data of the afm and the observer is implemented as an analog circuit as discussed above. A graphite sample was imaged with a set point amplitude $A_0$ equal to $90\%$ of free oscillation amplitude of $\approx$ 60nm with a scan size of $2\mu$m, proportional and integral gain $k_p = 0.2$ and $k_i = 0.4$ respectively and at different scan rates. The image of the sample at scan rate of 2 Hz is shown in Fig. 8(a). It can be observed that at this scan rate sub-nanometer features (of $\approx 0.6$ nm in height) of the graphite sample appear with approximately $0.1\mu m$ separation at scan position of $0.75\mu$m and $1\mu$m of the image. However the fine features disappear in the height image at scan rate of 16 Hz as seen in Fig. 8(b). In stead of edges of two layers of graphite on top of one another at the mentioned scan positions it appears as a smooth layer at the higher scan rate. In the amplitude image at scan rate of 16 Hz Fig. 8(c) the cantilever artifacts show up and the fine features on the sample are not manifested. However, the multiple graphite layers at scan positions of $0.75\mu$m and $1\mu$m are successfully detected at a scan rate of 16 Hz by using the decision rule from transient detection method [8] as shown in Fig. 8(c). Note that the cantilever is in transience during detection. In the experiment the sample layers in graphite correspond to detection bandwidth of 80 Hz at scan rate of 2 Hz and 640 Hz at scan rate of 16 Hz.

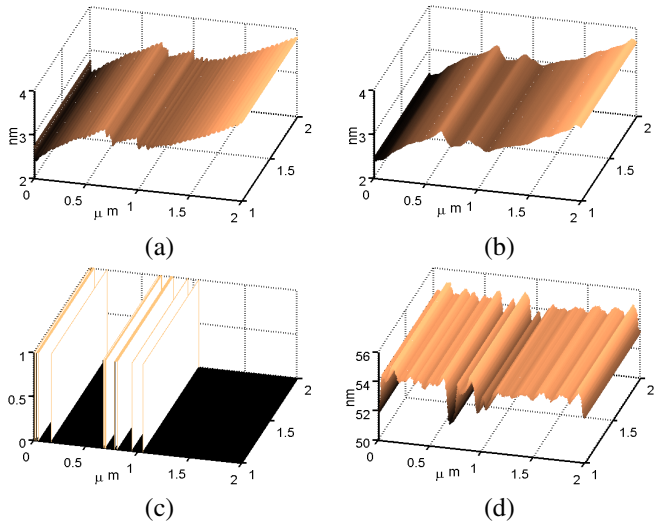


Fig. 8. (a) and (b) are the height images at scan rates of 2 Hz and 16 Hz respectively. (c) is the decision of sample detection at a scan rate of 16 Hz. (d) is the amplitude image at a scan rate of 16 Hz. At higher scan speed the height image becomes smooth and the graphite layers are lost. The decision rules shows detection of the graphite layers.

## IV. CONCLUSIONS AND FUTURE WORKS

### A. Conclusions

Observer based method provides an exact design and performance assessment for active $Q$ control in AFM. The transfer function from dither input to photo-diode output is independent of the observer so that the cantilever effectively behaves like a spring-mass-damper system unlike the complex behavior in existing methods. The effective quality factor and stiffness of the cantilever can be changed by appropriately choosing the state feedback gain. In an experiment the value of the $Q$ of a cantilever oscillating in water is enhanced to 350 from a nominal value of 5. The effect of tip-sample interaction force on the bandwidth and resolution during imaging is qualitatively analyzable in this framework. The observer provides flexibility in the state feedback loop to improve the bandwidth or resolution during imaging. It is observed from analysis and simulation that by appropriately choosing a slower state feedback loop the resolution of imaging can be improved when the cantilever is damped to have a higher bandwidth. Similarly the bandwidth of imaging can be improved when the $Q$ is enhanced to have a high resolution. This is remarkable improvement over the existing $Q$-control methods. The effect of noise on deflection signal is low when the cantilever is damped and the effect is severe when the $Q$ of the cantilever is enhanced. However the noise effect is less on the tip position estimate when a slower state feedback loop is considered. The transient detection scheme is married to observer based $Q$ control method during imaging. The transient detection scheme can be implemented independent of the estimated state feedback loop. In an experiment the transient detection scheme detected sub-nanometer ($\approx$ 0.6nm in height) features on a graphite sample spaced $\approx$0.1 $\mu$m apart at two different locations at a scan speed almost an order higher and the features were not distinguishable in the tapping mode images.

## REFERENCES


[1] G. Binnig, C. Quate, and C. Gerber, "Atomic force microscope," *Physical Review Letters*, vol. 56, no. 9, p. 930, 1986.

[2] T. Sulchek, R. Hsieh, J. Adams, G. Yaralioglu, S. Minne, C. Quate, J. Cleveland, A. Atalar, and D. Adderton, "High-speed tapping mode imaging with active q control for atomic force microscopy," *Applied Physics Letters*, vol. 76, no. 11, p. 1473, 2000.

[3] J. Tamayo, A. Humphris, and M. Miles, "Piconewton regime dynamic force microscopy in liquid," *Appl. Phys. Lett.*, vol. 77, no. 4, p. 582, 2000.

[4] F. Ohnesorge and G. Binnig, "True atomic resolution via repulsive and attractive forces," *Science*, vol. 260, p. 1451, 1993.

[5] P. Hansma, J. Cleveland, M. Radmacher, D. Walters, P. Hilner, M. Benzanilla, M. Fritz, D. Vie, H. Hansma, C. Prater, J. Massie, L. Fukunga, J. Gurley, and V. Eilings, "Tapping mode atomic force microscopy in liquids," *Applied Physics Letters*, vol. 64, p. 1738, 1994.

[6] C. Putman, K. V. der Werf, B. D. Grooth, N. V. Hulst, and J. Greeve, "Tapping mode atomic force microscopy in liquid," *Appl. Phys. Lett.*, vol. 64, p. 2454, 1994.

[7] R. D. Jäggi, A. Franco-Obregòn, P. Studerus, and K. Ensslin, "Detailed analysis of forces influencing lateral resolution for q-control and tapping mode," *Applied Physics Letters*, vol. 79, pp. 135–137, 2001.

[8] D. R. Sahoo, A. Sebastian, and M. V. Salapaka, "Transient-signal-based sample-detection in atomic force microscopy," *Appl. Phys. Lett.*, vol. 83, no. 26, p. 5521, 2003.

[9] T. R. Rodríguez and R. García, "Theory of q control in atomic force microscopy," *Applied Physics Ltters*, vol. 82, no. 26, p. 4821, 2003.